Journal of
Ship&Ocean
Technology
© MARCH 2000

SOTECH Vol. 4, No. 1, pp. 28~36 , 2000

Numerical Simulation of Directional Spreading Characteristics in a Snake Type Wave Generator considering Side Wall Reflection

Jin-Ho Lee[1] and Tsugukiyo Hirayama[2]

[1] Senior Researcher, Samsung Heavy Industries, Ltd, Korea; E-mail: realtiger@weppy.com
[2] Professor, Yokohama National University, Japan

Abstract

Numerical simulation based on the superposition of ring waves generated by the linear periodic source distributions for the plunger type wave maker was accomplished. The characteristics of directional spreading function were investigated. Mirror images are also introduced to consider reflections of side-wall together with the reflection coefficient to account for the imperfect reflection from the real side wall in the long experimental towing tank. Unexpected spurious waves, resulting from the combined effect of finite breadth of segmented wave maker, wavelength and main wave propagating direction, were observed in the line source method and also in the analysis of the directivity. The influence of spurious waves to the directional spreading function was also investigated.

Keywords: directional spreading function, spurious waves, line source method, directivity

1 Introduction

The generation of directional spectrum waves at the experimental tank has been demanded to simulate the behavior of ships or offshore structures in the real sea. The long towing tank at Yokohama National University has been successful in generating symmetric directional spectrum waves that have arbitrary spreading parameter(Takezawa et al 1988). Waves are generated by snake type segmented wave makers(the numbers of segments are 24 and the breadth of each is $0.3333m$) driven independently by servomotors at the end of the tank, with the side-wall wave absorbers lifted to get the reflection effect at the wall.

The nonlinear behavior of ships or floating offshore structures is affected by the directionality of the waves. Especially the breadth of the segmented wave maker is an important parameter to obtain the desirable directionality in this wave maker.

In this paper, we investigated the directionality dependence upon the breadth of wave maker applying the line source method.

Numerical generation of directional spectrum waves including side-wall reflection was explained in Section 2. To generate numerical directional spectrum wave field, we introduce periodic line sources representing each segment of wave maker and its image representing partial reflections at the side-wall by the reflection coefficient, $0 \leq \gamma \leq 1$. The wave field by imaginary wave

maker diminishes with increase of the imaginary tank index (m) proportional to γ^m. The results with finite reflection coefficient will be compared with those of perfect reflection($\gamma = 1$).

Desirable directional waves can be made theoretically by the sinusoidal motion of wave maker composed of infinite number of segments with infinitesimal breadth. In reality, the segmented wave maker can not have spatial sinusoidal or continuous motion due to the finiteness of the breadth. This limitation will make unexpected waves, called the spurious waves, to the directions other than that desired. The spurious waves are related to breadth of the plunger (Δb) in wave maker, wavelength (λ) and main wave direction (θ_0). We will investigate this phenomenon of the spurious waves using the line source method in Section 3.

The spurious waves will be compared with the result from directivity analysis, and their effects on the directional spectrum waves at the higher angular frequency in Section 4. These results will provide guideline on the design and control of the wave maker to generate desired wave fields in towing tanks. Section 5 summarizes the results.

2 Numerical simulation of directional spectrum waves

To calculate time series of wave elevation in long numerical wave tank, boundary integral method can be adopted. But this method needs a large number of meshes especially for short wavelength, and furthermore, the introduction of arbitrary reflection coefficient at side-wall seems difficult for long numerical tank. As similar method, velocity potential can be introduced using Green function explicitly satisfying perfect side-wall reflection(Kinoshita et al 1995, Isshiki 1975). In this paper, linear periodic source method is used explicitly to calculate directional spectrum waves(Hirayama and Lee 1996, Hirayama and Lee 1998). The advantages of this method are as follows. First of all, it is easy to get information at the arbitrary point where we want to get and make a dense mesh freely for the short waves. Secondly, the introduction of the reflection coefficient is more convenient than any other method. And, it is easy to consider the wave characteristics in the far field to develop generation of waves or make directional transfer function. We will therefore introduce this method to investigate wave characteristics and verify the usefulness of this method.

Directional spectrum waves, composed with line sources corresponding to each segmented wave generator and mirror images as side-wall reflection, will be represented as follows:

$$\zeta(x,y,t|\theta_0) = \sum_{j=1}^{J}\sum_{k=1}^{K} e^{-i(\omega_j t-\psi_{jk})}\frac{A(\omega_j,\theta_k)k_j}{\sqrt{2\pi g}} \left[\sum_{n=1}^{N}\sum_{m=-M}^{M}\int \gamma^{|m|}\sigma_0(l_{nm})\frac{1}{\sqrt{R}}e^{i(k_{0j}l_{nm}+k_j R)}dy'\right] \quad (1)$$

$$A(\omega_j,\theta_k|\alpha) = \sqrt{2S(\omega_j)D(\theta_k|\alpha)\Delta\omega\Delta\theta} \quad (2)$$

$$D_s(\theta_k|\alpha) = D_0\cos^{2n}(\theta_k-\alpha) \quad (3)$$

$$|\theta_k| \le \frac{\pi}{2}, \qquad D_0 = \frac{1}{\pi}\frac{2n!}{(2n-1)!} \quad (4)$$

where, ω(rad/s) is wave angular frequency, $g(m/s^2)$ acceleration of gravity, N total number of plungers in the span B of the wave maker, M number of reflection. Strength of source (σ_0) is

dependent on wave angular frequency according to the boundary condition of wave maker. $\gamma^{|m|}$ is reflection coefficient, R is a distance between any source point (0 , y). and reference point (x, y), $k_o = k \sin\theta_o$ is spanwise wave number of periodic moving plungers, l_{nm} is the distance of midpoint of each plungers numbered n, including m-th imaginary tank, k is wave number of propagating waves. ψ_{jk} is random phase of component wave having a uniform distribution. The amplitude of the component wave $A(\omega_j, \theta_k)$, assuming the separation of frequency spectrum and directional distribution, can be expressed as follows.

The shape of power spectrum of wave elevation $S(\omega_j)$was quoted from ITTC or ISSC model spectrum. As the component wave amplitude $A(\omega_j, \theta_k)$, we adopt the expression as shown in (2), (3) and we adopted, n=1 as a standard wind wave condition. Interval of angular frequency ($\Delta\omega$) should not be constant and preferable to be random variable to eliminate periodic reappearance of time series. Interval of wave propagating direction is selected as 5^o from the preparatory calculation. And α is main or principal direction of propagating wave, and in the case of long towing tank with side-wall, α is usually set to 0^o.

Depending on the index of the imaginary tank (m), θ_0 must be replaced as follows:

$$\theta_0 \rightarrow (-1)^m \theta_0 \quad \text{for} \quad -M \leq m \leq M \tag{5}$$

The spatial wave distribution and contour curves within 20 m from line source distribution was shown in Figure 1(a) and (b) without reflection effect and with one time reflection, respectively. Desired wave field was realized by increasing the number of imaginary tanks. This gives the broadening effect of the span of wave maker.

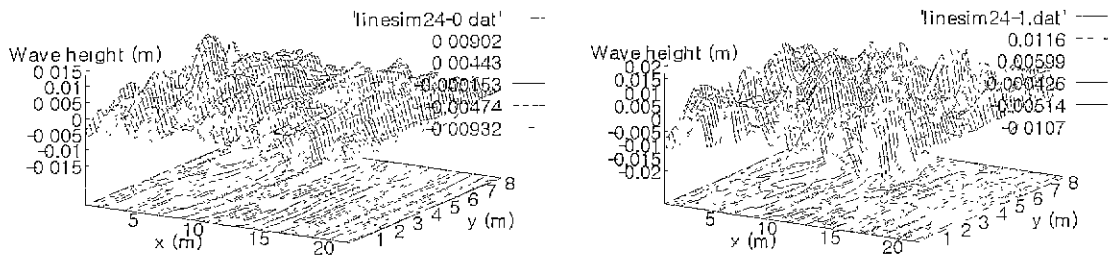

(a) (b)

Figure 1: Three dimensional numerical simulation of directional spectrum waves by the line source methods with the span B(ISSC, T_{01}=1s): (a) without reflection, (b) with one reflection on both sides of the tank

Propagating waves against real side-wall can not be reflected perfectly. So the influence of reflection coefficient γ on D_s must be evaluated. As examples, directional spreading function was evaluated corresponding to γ =0.6 in Figure 2(a). In order to see the effect of γ , D_s is estimated by varying the reflection coefficient as shown in Figure 2(b). As expected, peak of D_s becomes higher as γ reduces. D_s with γ =0.0 corresponds to the case without side-wall reflection.

This result will give us the least number of imaginary tank needed, because wave field by imaginary wave maker diminishes with increasing index of imaginary tank (m) in proportional to γ^m.

The summation of error between estimated directional spreading function and target function introducing perfect or partial reflection effect are shown in Figure 3(a) and (b). In these results, the directional spreading function considering perfect reflection was converged faster to the target distribution than that of considering partial reflection.

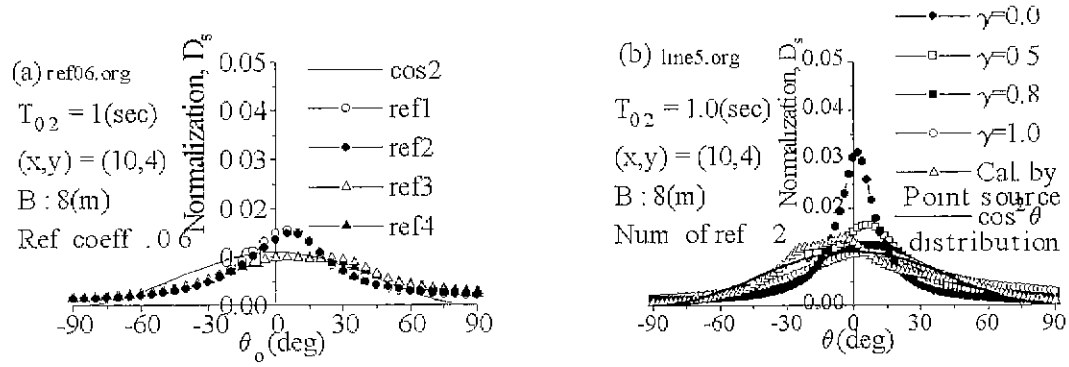

Figure 2: Wave spreading function D_s vs θ: (a) for various number of imaginary tanks with $\gamma = 0.6$, (b) for various reflection coefficient γ with $M = 2$

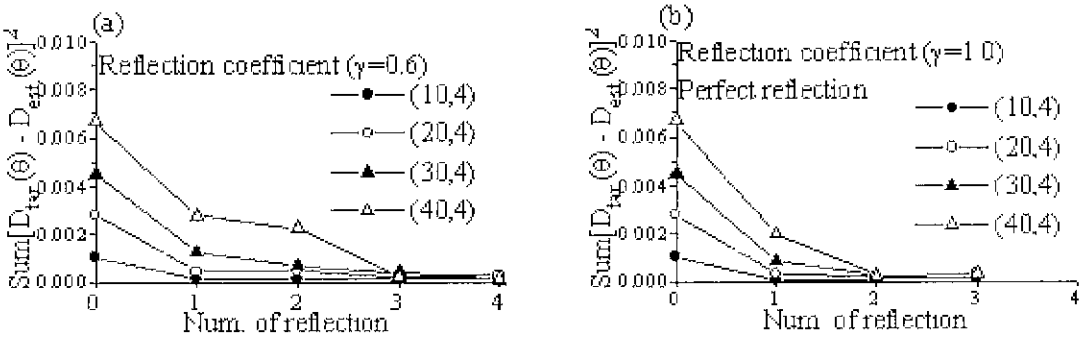

Figure 3: Summation of error between target D_s and estimated D_s: (a) partial reflection, (b) perfect reflection

3 Spurious waves in line source method

The perfect directional waves are obtained only with an infinitesimal width of plungers, i.e., the spatial motion of plunger should form a perfect sinusoid. The amplitude distribution of real wave

maker consisting of plungers of finite breadth is expressed as periodic step function. which causes the generation of spurious waves.

In this section, we will check the existence of spurious waves by varying the width of plungers Δb from $0.3333m$ to $0.16666\ m$ and at the same time doubling the number of plungers from 24 to 48 while keeping the span of wave maker ($B = 8\,m$) unchanged. Spurious waves will be generated in the direction of θ_p following (6):

$$\sin\theta_p = \frac{(-k_0\Delta b - 2\pi p)\lambda}{2\pi\Delta b},\ p = 0, \pm1, \pm2, \pm3, \cdots \tag{6}$$

Here, p denotes the number of spurious waves, the zero value corresponds to the main wave direction (θ_0). The range of p is as follows:

$$\frac{-k_0\Delta b}{2\pi} - \frac{\Delta b}{\lambda} \leq p \leq \frac{-k_0\Delta b}{2\pi} + \frac{\Delta b}{\lambda} \tag{7}$$

Thus, for a given wave direction (θ_0) and wavelength (λ), equation (7) gives the possible integer range for the spurious waves. When these values are used in (6), the actual spurious wave angle (θ_p) of all possible components can be found.

Spatial directional regular wave distribution from line source method is obtained by applying (8) and is shown in Figure 4(a) and (b).

$$\zeta(x, y, t|\theta_0) = e^{-i\omega t}\frac{k}{\sqrt{2\pi g}}\left[\sum_{n=1}^{N}\sum_{m=-M}^{M}\int \sigma_0(l_{nm})\frac{1}{\sqrt{R}}e^{i(k_0 l_{nm}+kR)}dy'\right] \tag{8}$$

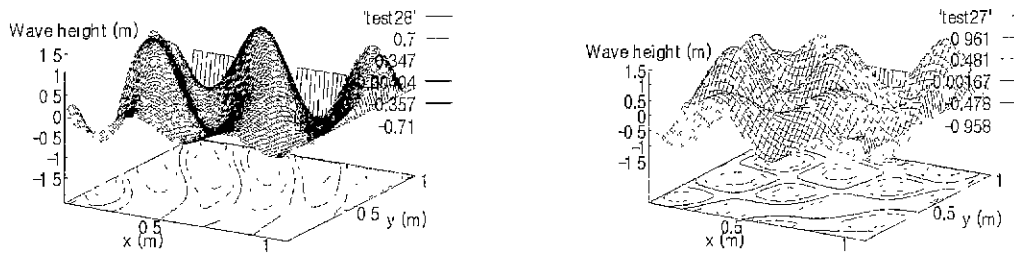

(a) (b)

Figure 4: Wave distribution by line source method with ω=12 rad/s, θ_o=30^o, B=8 m: (a) Δb=0.1666 m, number of plungers=48, (b) Δb=0.3333 m, number of plungers=24

High wave frequency, 12 (rad/s), was chosen to check the existence of the spurious waves corresponding to breadth of the segment, 0.1666 m(a), 0.3333 m(b). No spurious waves is observed in the case of the narrower segment(Figure 4(a)), whereas the spurious waves appear with the broader segment(Figure 4(b)). This implies that, once the spurious waves are present, the spatial wave distribution contains the wave component of undesirable direction.

4 Spurious wave in the analysis of directivity

In order to utilize the results developed in the antenna or acoustic field, we define the directivity. The directivity D_d means the distribution of wave amplitude propagating in θ direction in the far field from antenna or wave generator. In Figure 5, plan view and coordinate system of directional wave generator with side wall is shown. If the reference point (P) is so far from the origin, the variable distance (R) from each source point to reference point is approximately the same as to the distance (r) from the origin to reference point. It means that wave amplitude at the location far away from line source distribution should obey only propagating wave direction (θ) which is independent of the distance (R).

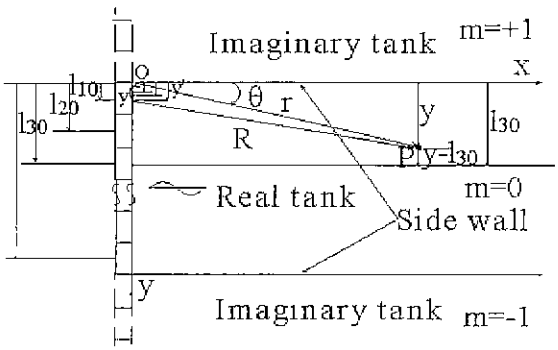

Figure 5: Coordinate system used for wave field generated by segmented wave makers

First of all, the relation between R and r can be represented as follows:

$$\begin{aligned} \overrightarrow{R} &= \overrightarrow{r} - y'\overrightarrow{j} = x\overrightarrow{i} + (y - y')\overrightarrow{j} \qquad (9) \\ R &= \sqrt{x^2 + (y - y')^2} \\ &= \sqrt{r^2\cos^2\theta + r^2\sin^2\theta - 2ry'\sin\theta + y'^2} \\ &= \sqrt{r^2 - 2ry'\sin\theta + y'^2} \qquad (10) \end{aligned}$$

which can be expanded in binomial series as:

$$R \simeq r - y'\sin\theta + \frac{y'^2}{2r} + \cdots \qquad (11)$$

The terms in this series decrease as the power of y' increases, if y' is small compared to r. In the denominator (which affects only the amplitude) of (8), we can drop the higher order terms as:

$$R \simeq r \qquad (12)$$

This approximation is valid in the far field, since r is very large compared to the tank width. The phase term kR in (8) should be treated more carefully in the directivity computation, since the distance R is multiplied by the wave number k. Although the amplitude of waves due to each source point is essentially the same, the phase may be different if the path length differences are a sizable fraction of a wavelength. We, therefore, include the first two terms of the series in (11) for R in the numerator of (8) giving

$$R \simeq r - y'\sin\theta \qquad (13)$$

The far field approximations (12) and (13) in (8) yields directivity (D_d) as follows:

$$\zeta(x, y, t|\theta_0) \rightarrow e^{-i\omega t} \frac{ke^{ikr}}{\sqrt{2\pi g\sqrt{r}}} D_d(\theta|\theta_0) \tag{14}$$

where

$$D_d(\theta|\theta_0) = \left[\sum_{n=1}^{N} \sum_{m=-M}^{M} \int \sigma_0(l_{nm}) e^{i(k_0 l_{nm} - ky' \sin\theta)} dy' \right] \tag{15}$$

From this, the directivity is obtained by the Fourier transformation of the distribution of $\sigma_0 e^{ik_0 l}$ and this is similar to the Kochin function in ship hydrodynamics.

Here, we introduce without far-field approximation D_ζ defined as follows:

$$D_\zeta(\theta|\theta_o) = |\zeta(x, y, t|\theta_0)| \equiv |\zeta(r\cos\theta, r\sin\theta, t|\theta_o)| \tag{16}$$

D_ζ is the wave amplitude distribution along (r, θ) points including the near field. So, θ is not always the direction of wave propagation in the near field.

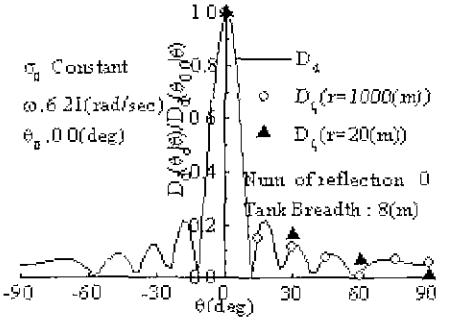

Figure 6: Comparison of directivity D_d with wave amplitude distribution D_ζ (D_ζ is computed using (16) and (8) for $r = 1000m$ and $r = 20m$.)

As described above, D_d, defined in the far field from line source distribution, is independent of the distance r. For example, normalized D_d (peak value is set to unity) calculated by (15) was compared with wave amplitude distribution in the far wave field $D_\zeta(r = 1000\,m$, and $r = 20\,m)$ computed with (16) and (8), for the specific wave frequency (ω = 6.21 rad/s) and specified wave direction (θ_0 =0.0 ^{o}) as shown in Figure 6. We see that D_ζ with $r = 1000\,m$ shows good agreement with D_d, but D_ζ with $r = 20\,m$ shows some deviation from D_d. This means that, in the near field, not only the behavior of wave field is different from that of far field, but also D_ζ does not express the waves propagating in θ direction.

The wave directivity by varying the width of plunger with wave angular frequency 12 rad/s and wave direction 30^o was represented in Figure 7. The spurious waves for the width of plunger $\Delta b = 0.3333\,m$ was shown in the direction about 51^o, but not for $\Delta b = 0.1666\,m$. This direction of spurious waves was approximately in an agreement with that of line source method in Figure 4(b).

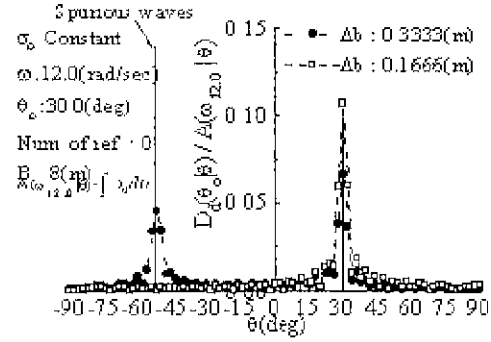

Figure 7: Directivity of line source distribution by varying the width of plungers. θ_0=30^o, Δb=0.3333, Δb=0.1666; Vertical lines show the theoretical position of spurious waves

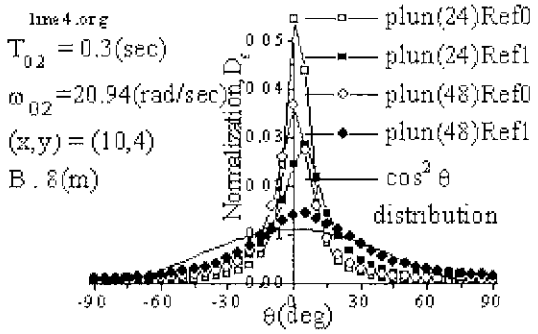

Figure 8: Wave spreading function by varying the number of segments in wave maker (Span of wave maker is fixed)

Directional spectrum estimated from time series of waves expressed by (1) by varying the width of plunger and side-wall reflection are shown in Figure 8. Although the frequency is relatively high in this case, the effect of spurious waves is not clearly observed. One reason will be that the finite truncation of ω- and θ-summations in double or single summation method is not sufficient to verify the existence of spurious waves.

Estimated directional spectrum waves by 48 plungers of 0.1666 m width and with side-wall reflection has higher fidelity to the target D_s than those by 24 with 0.3333 m width.

5 Conclusions

Generation of directional spectrum wave is studied with the results as follows:

(1) Estimated directional spreading characteristics of multi-directional irregular waves made by linear superposition of velocity potential, considering the characteristics of snake type wave generator, and side-wall reflection by imaginary tanks, showed good agreement with target

function near the wave maker. To maintain the same directional resolution in far fields as in the near fields, more reflection or imaginary tanks are needed.

(2) Side-wall reflection has the effect of making total wave maker span broader, and hence by increasing the number of imaginary tanks, generated results approach to the desired spreading function.

About spurious waves

(3) From the line source method, we confirmed that the spurious waves are generated in the directional regular waves due to the finite width(Δb) of segments of the wave maker. But, these waves are not observed clearly in the directional spectrum waves, due to the finiteness in the numbers of frequencies and directions in the single or double summation method. The spurious waves are considered merged together and hence are not detectable.

References

HIRAYAMA, T. AND LEE, J.H. 1996 Simulation of multi-direction irregular waves and wave forces acting on structures composed of slender members. Korea-Japan Joint Workshop on Ship and Marine Hydrodynamics, Korea, pp. 370-377

HIRAYAMA, T. AND LEE, J.H. 1998 Directional wave characteristics of multi-directional wave generator based on numerical simulation. J. of Society of Naval Architects of Japan, **184** , pp. 83-94

ISHIDA, S. 1996 Properties of oblique long crested irregular waves by snake motion of segmented wavemaker.

ISSHIKI, H. 1975 Water Waves in a Long Canal - The velocity potential of a periodic source. J. of Society of Naval Architects of Japan, **137** . pp. 34-47

KINOSHITA, T. ET AL 1995 Effects of measuring positions on directional wave spectrum in a basin side with side-wall reflection. Wave Generation 95 Yokohama, Japan, pp. 83-105

STIG, E.S. 1986 Directional wave generation. Joint seminar of the IAHR working group on wave generation and the ITTC, Holland

TAKEZAWA, S., KOBAYASHI, K. AND KASAHARA, A. 1988 Directional irregular waves generated in a towing tank. J. of Society of Naval Architects of Japan, **163**, pp. 222-232

STUTZMAN, W.L. AND TIESLS, G.A. 1981 Antenna Theory and Design. John Wiley & Sons Inc.